Fabrication and characterization of a micromachined deformable mirror for adaptive optics applications

Linda M. Miller
William J. Kaiser
Thomas W. Kenny

Microdevices Technology Section, Jet Propulsion Laboratory, California Institute of Technology, Pasadena, CA 91109

Michael L. Agronin

Guidance and Control Section, Jet Propulsion Laboratory, California Institute of Technology, Pasadena, CA 91109

Robert L, Norton

Applied Mechanics Technologies Section, Jet Propulsion Laboratory, California Institute of Technology, Pasadena, CA 91109

ABSTRACT

A novel micromachined electrostatically controlled deformable mirror has been fabricated and characterized which uniquely combines the fields of microinstruments, adaptive optics and controls to form a silicon-based mirror assembly that is relatively simple to process, inexpensive, lightweight, and integrable with drive and sensing electronics. Electrostatic control of a thin membrane mirror is demonstrated with low voltage actuation and without the need for complex construction of PZT, or other translator-type arrays. In addition, the low-stress Si-rich Si_xN_y film used as the deformable membrane mirror is thermally matched to the silicon supporting frame. Custom design of the mirror shape can be implemented by simply redesigning the electrode pattern on an insulating substrate separate from the thin film mirror. Test results from a pull-only circular mirror with a single pixel actuator are presented as a proof of concept for low voltage actuation of a low-stress Si_xN_y flexible membrane. Finite difference modeling of the structure is utilized to calculate an initial stress of 668 MPa for the tensily stressed Si_xN_y membrane. This is in contrast

to the value of 150 MPa that was measured with the wafer bowing method. (This discrepancy is being addressed in on-going research of this device.) This tensile stress increases the voltage required for deflection of the membrane, but insures a linear relationship between the center deflection of the mirror and the applied pressure. This significantly simplifies the controls algorithm required for closed-loop operation of this device,

1. INTRODUCTION

As the desire for more accurate and inexpensive optical science grows, driven by programs such as Toward Other Planetary Systems (TOPS), we've identified a growing need for active and adaptive optical elements. Applications range from controlling a few degrees of freedom (tip and tilt, or piston) to correcting static or thermally-induced misalignments in optical systems, to dynamically controlling hundreds of degrees of freedom to correct atmospheric aberrations for large telescopes. In this work, a rnicromachincd, electrostatically controlled and capacitively sensed deformable membrane mirror is proposed to meet these needs.

Membrane mirrors have been investigated [1-9] as active and adaptive optics elements because of their large deflection range, their relative ease of fabrication, and the simplicity of actuation (either by means of variable pressure or electrostatic actuation). A typical method in fabricating deformable membranes has been [1-5] to stretch a thin reflective film across a circular frame and control the shape of the mirror either with piezoelectric or electrostatic actuators, Although impressive operation has been obtained with these designs, the assembly is complex and a considerable effort is required to insure the thermal stability of these devices. Micromachined membranes have also been investigated[6-10] as controllable diaphragms in applications such as beam focusing, spatial light modulators and infrared detectors. To date, however, the dimensions of these devices have been small and the applications have been limited in scope. In the work presented herein, micromachined thin films are combined with electrostatic control to form an adaptive optical element that is relatively simple to process, inexpensive, lightweight, and integrable with drive and sensing electronics.

In this paper, the theory, fabrication and test results of a flat, clamped circular membrane mirror are discussed. The nonlinear theory of membranes is presented first in Section 2. Electrostatic control of the deformable membrane mirror and the relationship between pressure and applied dc bias arc also discussed. "l-he fabrication of the micromachined mirror assembly is described in Section 3. Detailed processing is discussed for the free-standing reflective membrane and the patterned drive electrode plate. The flip-chip configuration described in this section is

utilized to reduced the drive voltage required by reducing the gap spacing between the membrane mirror and the drive electrode. In Section 4, interferometry test results are presented which characterize the initial flatness of the membrane mirrors and the functional dependence of deflection on applied bias. Center deflection data is used to derive an initial stress of 668 MPa in the Si-rich Si_xN_y films. This value is significantly higher than the 150 MPa value measured using a bowing wafer measurement.[15] Future research areas are discussed in the Conclusion Section which include the measurement of the resonant frequency of the membrane to confirm the tensile stress in the membrane, the upscaling of the membrane dimensions to reduce drive voltage requirements, and the inclusion of a multi-pixelated drive electrode array for the correction of higher order Zernike terms.

2. THEORY

In determining the controls algorithm for closed-loop operation of the Si_xN_y membrane mirror, the functional form of center deflection as a function of applied pressure, P, is required. Theoretically, a flat, circular, clamped membrane approximates the shape of a shperical shell when a uniform pressure is applied. The functional relationship between the uniform pressure anti the center displacement , y, of the membrane is of the form [16]:

$$\frac{P a^4}{Eh^4} = \frac{16}{3(1-\nu^2)}\left(\frac{y}{h}\right) + \frac{(7-\nu)}{(3(1-\nu))}\left(\frac{y}{h}\right)^3 \quad (1)$$

where a is the radius of the membrane, E (= 3.85 x 107 N/cm)[14] is Young's modulus of Si3N4, h is the membrane thickness and v (= 0.279)17 is Poisson's ratio. For small deflections (deflections less than about half the thickness of the membrane), the left term of Equation 1 is dominant and the deformation of the membrane is linear with applied pressure. For large deflections, the right-most term dominates and the deflection becomes a nonlinear function of pressure. Operating in this regime is requires a significantly more complex controls algorithm than for a system which is strictly linear.

For a conductive membrane controlled electrostatically, the pressure, P [Pa], is related to the applied voltage by

$$P = \frac{1}{2}\frac{\varepsilon_0}{d^2}V^2 \quad , \quad (2)$$

where ε_0 is the permittivity of air, d is the gap spacing between the membrane and the drive electrode, and V is the drive voltage. In this expression, the gap change with applied pressure is assumed to be small with respect to the total gap spacing, d.

Combining these expressions, the voltage required for a center displacement of y is

$$V^2 = \frac{d^2}{a^4}(\alpha y + \beta y^3) \tag{3}$$

where α and β are constants determined by the material parameters and the dimensions of the membrane. Note that the voltage required for a given center deflection of the membrane can be greatly reduced by increasing the diameter of the circular membrane and by reducing the gap spacing. Obviously there are constraints to these design parameters. For example, it has been shown[18] that at a center deflection of one third the gap spacing, the membrane will collapse onto the opposing electrode. This constrains the gap spacing to three times the maximum center deflection required for a particular application. Likewise, increasing the diameter of the membrane may significantly decrease the yield of the process. These design considerations will be applied in the characterization of the mirror deflection as a function of drive voltage is Section 4.

3. FARRICATION "'

The pull-only micromachined, electrostatically controlled deformable mirror assembly is shown schematically in Figure 1. The membrane mirror consists of a low-stress, Si-rich SixNY,[11-13] circular membrane (thickness = 0.5 μm, diameter = 8 mm) supported by a silicon frame. Si-rich Si_xN_y was selected as the membrane material because it can be fabricated with an initial tensile stress that insures an initially flat mirror provided that the silicon frame is also optically flat. Si-rich Si_xN_y is also thermally matched to the silicon and acts as an excellent etch-stop layer[14] for wet-chemical etches such as EDP and KOH which are commonly used in the fabrication of other microinstruments. Electrostatic control of the membrane mirror shape is achieved by applying a dc bias across the opposing electrode, labelled V_{bias}, and the grounded membrane. The gap spacing between the electrodes, labelled d in Figure 1, is controlled by the depth of the well etched into the dielectric plate which supports the bias electrode. Although some assembly is required in this design, simple alignment marks are incorporated into the metallization pattern of the electrode array to facilitate alignment, as discussed below. In addition, the membrane mirrors can be mass-produced and specific applications can be accommodated with a custom design of the electrode array. This configuration also allows for insitu capacitive sensing of the membrane displacement

with silicon-based electronics that can be integrated with the mirror assembly to minimize the effects of stray capacitances and thermal noise. The details of the micromachining follow.

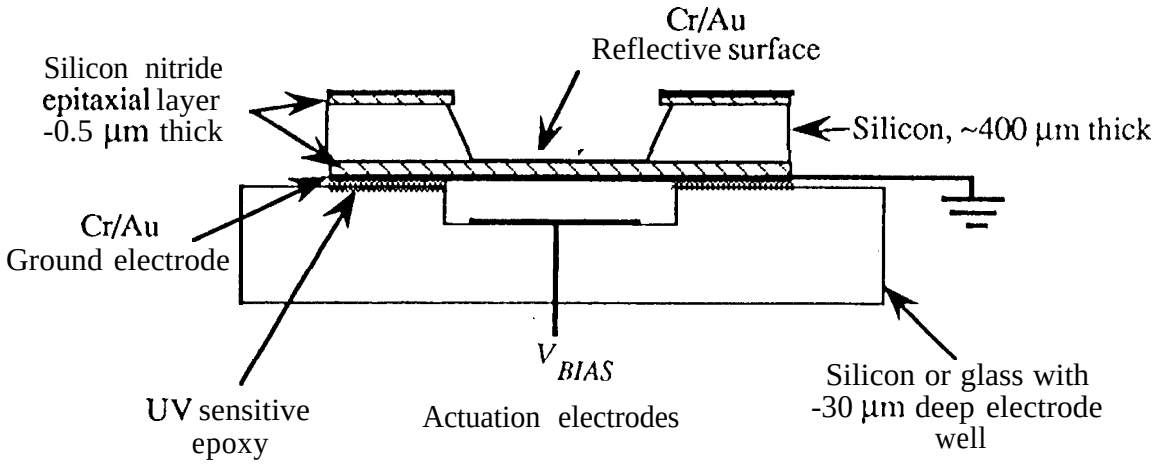

Figure 1. Schematic view of the cross-section of a push-pull, micromachined, electrostatically controlled, capacitively sensed deformable mirror.

The micromachined deformable mirror assembly characterized herein was micromachined from a 7.6 cm diameter silicon substrate (-400 μm thick) polished on both sides with a standard semiconductor-grade polishing procedure. A thin film (-0.56 μm) of low-stress, Si-rich Si_xN_y was deposited on both sides of the silicon wafer at which time the initial tensile stress in the film was measured at 150 MPa using a substrate bowing technique. [15] The coated silicon wafer was then processed using bulk micromachining technology as shown schematically in Figure 2. The membrane side of the wafer was first coated with Cr/Au (-50 nm) to protect the $SixN_y$ during processing and to act as a drive electrode in the final assembly. Standard photolithographic techniques and dry-etching were then utilized to open 8 mm diameter circular windows with a 1 mm wide supporting rings into the Si_xN_y etch mask (top Si_xN_y layer in Figure 2a). Ethylene diamine, pyrocatechol, and water (EDP) was then used to etch through [he silicon wafer, as shown in Figure 2b. Finally, the backside of the wafer was coated with Cr/Au (-50 nm) to produce the reflective surface of the membrane mirror (Figure 2c).

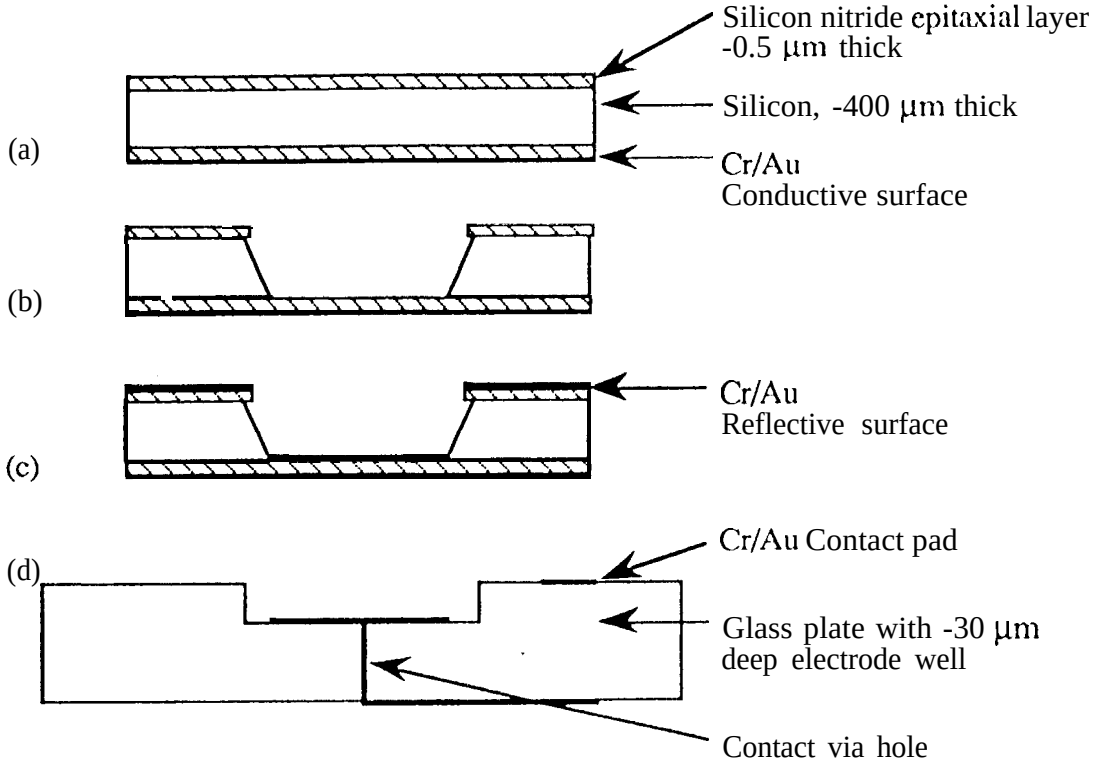

Figure 2. Fabrication steps of the micromachined deformable mirror assembly. (a) A polished silicon wafer is coated on both sides with low-stress Si-rich Si_xN_y. One surface was coated with Cr/Au to form the contact to the membrane mirror. (b) Photolithography, dry etching and bulk micromachining were used to define the boundary and supporting ring of the clamped circular membrane. (c) Cr/Au was deposited on the exposed surface of the membrane to form the reflective surface. (d) The drive electrode plate was fabricated using photolithography, isotropic wet chemical etching and Cr/Au evaporation, Contact via holes were fabricated using a 0.75 mm diamond coated cutting tool.

The back electrode plate was fabricated from an insulating glass plate. A thick Cr/Au film (-10 nm Cr, -400 nm Au) was deposited onto surface of the glass plate and patterned using standard photolithographic techniques. Flat circular wells, ~8 mm in diameter, were isotropically etched to a depth of 20 μm and 30 μm into the glass using a dilute HF mixture. Via holes through the glass plate were then fabricated using a 0.75 mm diamond coated cutting tool. Cr/Au was again deposited onto the etched surface and patterned to produce electrically isolated drive electrodes and contact pads for the membrane mirrors. Drive electrode pads were fabricated into 8 mm diameter circles which were contacted through the via holes using silver paint.

The membrane mirrors were assembled in a flip-chip configuration as shown in Figure 1. Alignment marks incorporated into the metallization pattern for the single pixel electrodes were used to align the membrane mirror to the back electrode plate and contact to the membrane was made with the contact pads described above. Finally, UV sensitive epoxy was used to glue the mirror to the drive electrode plate.

4. CHARACTERIZATION

In this section, interferometric data is used to characterize the initial flatness and functional dependence of center deflection on drive voltage for several mirror assemblies, The factors influencing the initial flatness of the membrane mirror are first addressed in Section 4.1. These factors include stresses incurred from the UV epoxy and the deposition of different metal thicknesses on either side of the membrane, and the field induced from the charging of the Si-rich SixNY. In Section 4.2, center deflection as a function of dc drive voltage is characterized and compared to the membrane model presented in Section 2. The effect of the total gap spacing between the membrane mirror and the single pixel drive electrode is also analyzed. Finally, an initial tensile stress of 668 MPa in the Si-rich Si_xN_y is calculated from deflection data using a finite difference model.

A Zygo Mark IV interferometer (λ = 633 nm) and a low current dc power supply were used to characterize the devices discussed in this section, In all cases, the membrane was grounded and a dc voltage was applied to the corresponding single pixel drive electrode. Reflectance fringe data was analyzed and converted to peak-to-valley data and radius of curvature data. In the evaluation of the initial flatness of the membranes, peak-to-valley data was used as the figure of merit. As dc bias was applied, however, the interferometer was unable to resolve the closely-spaced fringes at the periphery of the membrane and the radius of curvature was used instead to determine the center deflection value.

4.1 Flatness

An initially flat mirror is expected in the micromachined deformable mirror for the ideal case of an optically flat and rigid frame, uniform gluing to the electrode plate and a slightly tensily stressed membrane. In the devices presented in this section, however, the flattest mirror has a measured peak-to-valley value of 0.5λ with a large center area that is flat to $<\lambda/10$. This device is affixed loosely (no epoxy) to the mirror holder in the test set-up, and has equal thicknesses of metal on both surfaces of the membrane. Peak-to-valley values increase with the addition of epoxy

(0.6λ to 1.0λ), nonequal thicknesses of metal on both sides of the membrane and epoxy (1.3λ to 1.8λ), and charging of the Si-rich Si_xN_y (8λ). Charging effects in the Si-rich Si_xN_y have been extensively documented. [18-19] However, by metallizing and grounding the back surface of the membrane, this problem is alleviated.

A typical initial shape for the membrane mirrors tested here is shown in Figure 3a. Although the membranes are tensily stressed, the shape of the starting wafer determines the initial shape of the mirror. Shown in Figure 3b is an interferogram of a similar silicon wafer of the same thickness as that used in the fabrication of deformable mirrors. Nonuniformities as much as 6λ are observed across a 8 mm lateral dimension. These nonuniformities are incurred during the polishing of thin silicon wafers, but can be eliminated by optically polishing a thick silicon wafer. Fabrication of thick silicon wafers which have been optically polished to λ/10 is currently in progress.

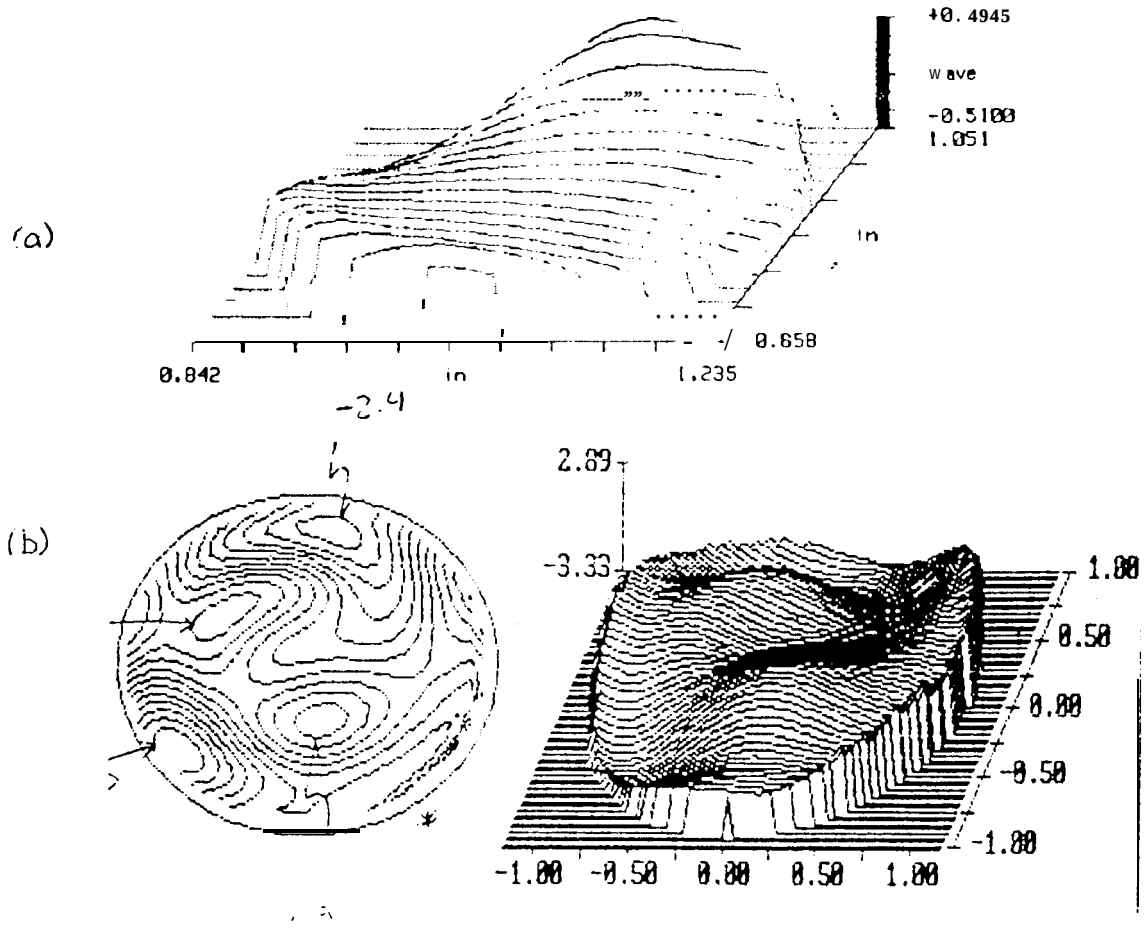

Figure 3. Interferometric data for (a) an 8 mm diameter, circular membrane mirror assembly with zero applied bias, and (b) a 33 mm diameter circular section of a 76 mm diameter, 400 μm thick silicon wafer.

4.2 **Deflection vs Voltage**

Interferometry is also utilized to determine the center deflection of the circular membranes with increasing dc voltage applied across the drive electrode and the grounded membrane. At large biases, however, the interferometer is unable to resolve the closely spaced fringes at the periphery of the membrane. Therefore, the radius of curvature data is a more appropriate measure of center deflection as a function of drive voltage. Assuming an approximately spherical shape of the membrane, as discussed in the theory section, the functional relationship between the center deflection, y, and the radius of curvature, R, is

$$y = \frac{d^2}{8R}, \tag{4}$$

where d = 8 mm is the diameter of the membrane.

Deflection as a function of dc drive voltage is shown in Figure 4 for two membrane mirrors with equal thicknesses of metal on either side of the membranes. The gap spacing between the single pixel drive electrode and the membrane mirror is 20.0 μm and 29.5 μm for the devices labelled A and B, respectively. Also shown in Figure 4 is the predicted profile for Device B, given the relationship expressed in Equation 3, i.e. the ratio between the two curves should correspond to the ratio of the gap spacings. The discrepancy between the actual and predicted profiles for Device B is attributed to its elliptical shape as it is deformed. Device E more closely approaches a shperical shape. However, as demonstrated by Figure 4, the drive voltage is clearly reduced by reducing the gap spacing between the membrane and the drive electrode.

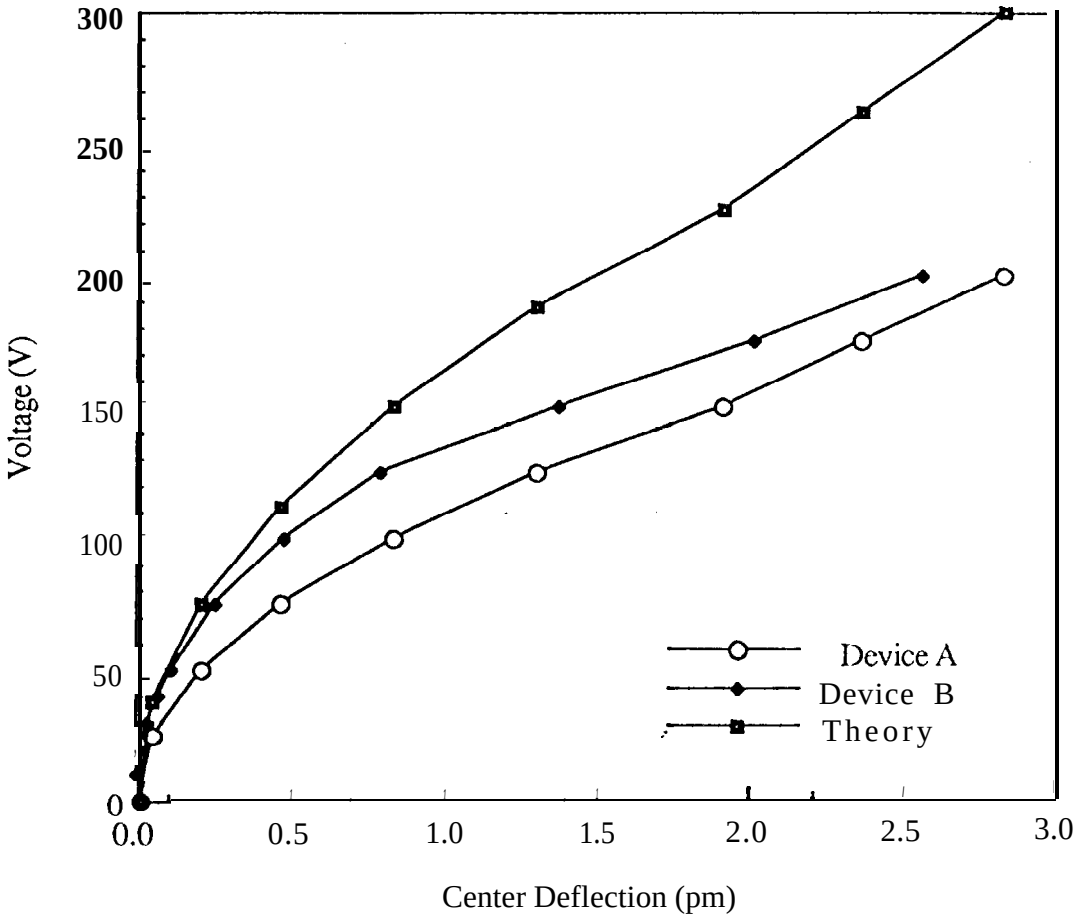

Figure 4. Functional relationship between drive voltage and center deflection for two clamped, circular membrane mirror assemblies. Device A has a gap spacing of 20 μm. Device B is identical with the exception of a gap spacing which is 30 μm. The curve marked theory is the predicted profile for Device B given the profile of Device A.

In examining the relationship between deflection and applied voltage further, the predicted profile of the flat, clamped, circular membrane model from Equation 3, is plotted together with the deflection profile of Device A (gap spacing= 20 μm) in Figure 5. At the largest deflection of 2.83 μm, the actual voltage required is ~75 times that predicted by the membrane model. Clearly, the

model is inappropriate for the devices tested here. For this reason, another approach was pursued using a finite difference model to determine the amount of initial stress in the Si_xN_y membranes prior to actuation.

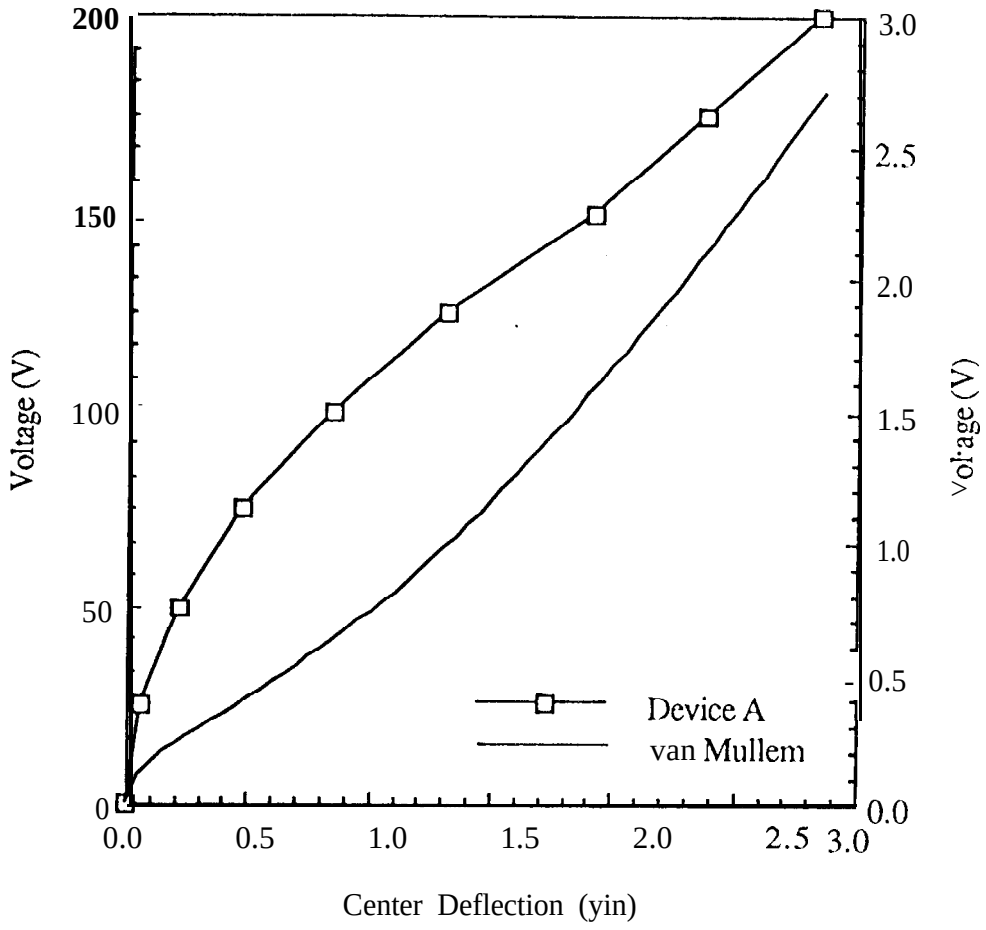

Figure 5. Voltage as a function of center deflection for a membrane mirror with a gap spacing of 20 μm and the predicted profile for an identical device as predicted by the flat, clamped, circular membrane model of Equations 1-3.

The alternative approach used in this analysis is that of the finite difference method in solving the well known differential equation for an axisymmetric membrane with lateral pressure:

$$\frac{dw}{dr^2} + \frac{1}{r}\frac{dw}{dr} = -\frac{P}{T}, \quad (5)$$

where w is the membrane displacement, r is the membrane radius, P is the pressure applied to the membrane, and T is the tension in the membrane. The solution can be easily obtained for the case of uniform pressure and constant tension. This solution is appropriate for cases where the initial tension is large and the tension does not change with the lateral deflection, w. In case of the deformable mirror, the assumption is that the membrane tension changes substantially with deflection.

To solve the case with varying membrane tension, finite difference techniques are used to solve the differential equation (Equation 5). First, the differential equation is approximated by differences in the lateral deflection from node point to node point on the membrane surface. Then, the starting tension, supplied from the wafer bowing measurement, and some amount of the applied pressure (load step) is used to compute the membrane deflection. From the membrane deflections, the change in membrane length is computed, and from the change in length a modified membrane tension is computed. This new tension is used to re-compute the lateral deflections. This process is iterated until a self-consistent pretension value is produced. Next the load step is incremented, and the iteration is done until the equation has converged at this load step. The load steps are repeated until the. final load is achieved,

The predicted values of deflection as a function of pressure are plotted with device A in Figure 6, where voltage data from Figure 4 has been converted to pressure using equation 2. From this plot, it is clear that the deflection is linear with applied pressure. Therefore, Equation 5 can be used to determine the initial stress 668 MPa. This value is clearly larger than the measured value of 150 MPa produced from the bowing wafer technique. Work is currently in progress to confirm this value by measuring the resonant frequency of the deformable membrane.[20]

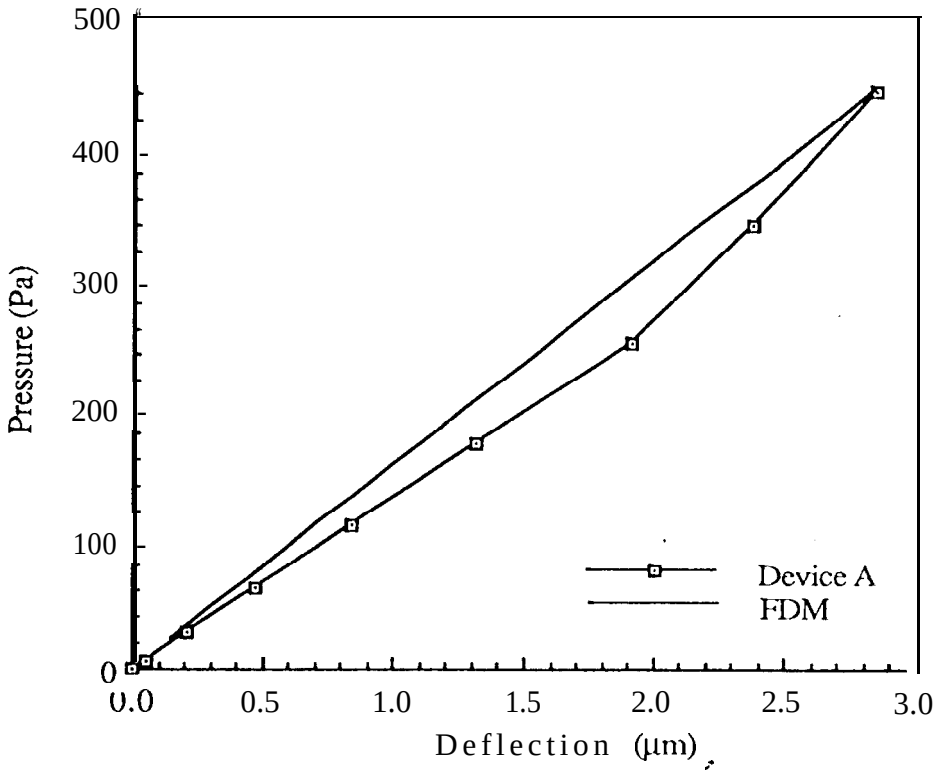

Figure 6. Applied dc voltage as a function of center deflection for device A and the finite difference method calculation for an identical device.

5. CONCLUSION

A micromachined deformable mirror consisting of a Si-rich Si_xN_y membrane mirror and an opposing single pixel drive electrode has been designed, fabricated and characterized, Bulk micromachining and standard photolithographic techniques are utilized to fabricate both the free standing membrane mirror and the patterned dielectric electrode plate. Alignment of the mirror and electrode is incorporated into the design of the single electrode pattern. Electrostatic control of the membrane mirror is achieved by grounding the metallized membrane mirror and applying a dc drive voltage across the membrane and drive electrode.

Devices are characterized by the initial flatness of the membrane mirror and the amount of deflection produced by a given dc bias voltage. Both characteristics are measured using a Zygo Mark IV interferometer. Initial flatness to 0.5λ (λ = 633 nm) has been achieved with standard

silicon polishing of a thin silicon wafer and no gluing. Optimization of the mirror flatness is proposed by utilizing thick silicon wafers with optically polished surfaces. Center deflection of the circular membrane mirrors is found to increase with decreasing gap spacing between the membrane and the drive electrode, however, the deflection is considerably less than that predicted by the flat, clamped, circular membrane model. A finite difference method is applied to the data to calculate an initial tensile stress of 668 MPa of initial stress in the membrane. 'I'his value is used then used to calculate the deflection profile of the membrane. This value is in contrast to the value of 150 MPa determined by the wafer bowing method and is currently being researched.

Deflections on the order of 2.8 μm with 200 V of applied bias was achieved for devices with gap spacing between the membrane mirror and the drive electrode of 20 μm. Using the scaling factors of Equation 3, the voltage required for the same center deflection of a 2,5 cm diameter circular membrane should be on the order of 2 V.

Future research will focus on the optimization of the initial flatness of the membrane mirror as well as the scaling of the dimensions of the membrane mirror to 2.5 cm diameter. With this larger diameter, a prescribed electrode pattern can be utilized to accommodate second order Zernike corrections of the optical train.

7. ACKNOWLEDGMENTS

The authors thank R. K. Bartman for his contribution in the conceptual work of this project. The authors also wish to thank F. Y. Hadaegh and P. K. C. Wang technical support in the controls aspects of the device design. The work described in this paper was performed by the Microdevices Technology Section, Jet Propulsion Laboratory, California Institute of Technology and is sponsored by NASA Code R (232-61013-0343).

8. REFERENCES

1. V. V. Motoshkin and S. M. Slobodyan, "Spectral properties of varifocal membrane mirror, "

2. R. P. Grosso and M. J. Yellin, "The membrane mirror as an adaptive optical element, " *J. Opt. Sot. Am.,* Vol. 67, pp. 399-406, 1977.

3. F. Merkle, K. Freischlad and H.-L. Reischmann, "Deformable mirror combined peozoelectric and electrostatic actuators, " *SPIE*, Vol. 332, pp. 260-268, 1982.

4. I.. J. Hornbeck, " 128 X 128 Deformable mirror device, " *IEEE Trans. Electron. Dev.*, Vol. ED-30, pp. 539-545, 1983.

5. M. Harada, "Variable-focus concave mirror utilizing single crystal Si diaphragm (in Japanese)," *Proc. IEE Japan*, Vol. 6, pp. 163-164, 1989.

6. H. H. Jerman, "The fabrication and use of micromachined corrugated silicon <diaphragms," *Sensors and Actuators,* Vol. A21-A23, pp. 988-992, 1990.

7. M. A. Ealey, "Active and adaptive optical components: The technology and future trends," *SPIE*, Vol. 1543, pp. 2-38 (?), 1991.

8. C. J. van Mullem, K. J. Gabriel AND H. Fujita, "Large deflection performance of surgace micromachined corrugated diaphragms, ". ????. Vol. ???, pp. 1014-1017, 1991.

9. M. Hisanaga, T. Koumura and T. Hattori, "Fabrication of 3-dimensionally sahped Si diaphragm dynamic focusing mirror," *Proc. IEEE Mirco Electro Mechanical Systems (iMEMS),* Ft. Lauderdale, FL, pp. 30-35, Feb. 7-10, 1993.

10.1'. W. Kenny, W. J. Kaiser, J. K. Reynolds, J. A. Podosek, H. K. Rockstad, E. C. Vote, and S. B. Waltman, "Electron Tunnel Sensors," *J. Vat. Sci. Technol. A,* Vol. 10, pp. 2114-2118.

11. V. V. Voskoboynikov, V. A. Gritsenko, N. D. Dikovskaya, B. N. Zaitsev, K. P. Mogilnicov, V. M. Osadchii, S. P. Sinitsa and F. L. Edelman, "Strucutre, optical and electrical properties of silicon-rich silicon nitride films" *Thin Solid Films (Switzerland),* Vol. 32, pp. 339-342, 1976.

12. C. Kaya, T.-P. Ma, T.-C. Chen and R. C. Barker, "Properties of Si-rich SiN_x:H films prepared by plasma-enhanced chameical vapor deposition," *J. Appl. Phys.*, Vol. 64, pp. 3949-3957, 1988.

13. B. Reynes and J. C. Bruyere, "nigh-density silicon nitride thin film in PECVD," *Sensors and Actuators A,* Vol. 32, pp. 303-306, 1992.

14. K. E. Peterson, "Silicon as a mechanical material," *Proc. IEEE,* Vol. 70, pp. 420-451, 1982, and references therein.

15. A. Brenner and S. Senderoff, *J. Res. Natl. Bur. Stand.,* Vol. 42, pp. 105-, 1949.

16. M. Di Giovanni, Flat and Corrugated Diaphragm Design Handbook, Marcel Dekker Inc., New York, 1982.

17. Properties of Silicon, emis datareviews series No. 4, INSPEC, The Institute of Electrical Engineers, London and New York, 1988.

18. D. A. Buchanan, R. A. Abram and M. J. Morant, "Charge trapping in silicon-rich Si_3N_4 thin films," *Solid-State Electron.*, Vol. 30, pp. 1295-1301, 1987.

19. W. S. Lau, S. J. Fonash and J. Kanicki, "Stability of electrical properties of nitrogen-rich, silicon-rich, and soichiometric silicon nitride films," *J. Appl. Phys.*, Vol. 66, pp. 2765-2767, 1989.

20. W. C. Young, Roark's Formulas for Stress and Strain, Sixth Ed., McGraw-Hill Inc., New York, 1989.